

Comparison of Fragment Formation Techniques for the Dynamics of Au-Au Collisions at 35 MeV/Nucleon.

Dr. Supriya Goyal

Submitted: 26/04/2023 Revised: 27/06/2023 Accepted: 15/07/2023

Abstract: The impact of fragment formation techniques on the dynamics of central to most peripheral $^{197}\text{Au}+^{197}\text{Au}$ collisions at low excitation energy of 35 MeV/nucleon is studied using Quantum Molecular Dynamics Model (QMD). We compared the final stage multiplicity of various fragments, charge yields, and distributions of light and intermediate charge fragments in velocity space with six different types of fragment formation techniques commonly known as clusterization methods. Our results clearly show a significant effect of fragment formation methods on the various quantities. Comparison with experimental data is also presented in some cases.

Keywords: heavy-ion collisions, fragment formation, multifragmentation, charge-yield

1. Introduction

One of the complex phenomena under extensive study in intermediate energy heavy-ion collisions is named as “Multifragmentation” [1-3]. Different types of dynamical [4,5] and sequential/statistical [6] approaches are used to study these phenomena [7,8]. The generated phase space by dynamical approach is clubbed with decay processes in order to investigate the fine structure of the produced fragments [8]. In Ref. [9] it is even shown that de-excitation processes used at the last stage are not even required to reproduce various properties. In the present study, discussion is limited to dynamical approach where development of reaction is taken care from start till the point where well separated fragments are produced. Various fragment formation secondary techniques are used to identify the fragments formed from the phase space of nucleons. Fragmentation from reaction and spectator zone, universality behavior and phase transitions in emission of fragments at high energies are observed in the literature [1-9]. However, little is known about the reaction kinetics and related non-equilibrium features in low-energy heavy-ion collisions [10]. Whether a nuclear

system may achieve thermal equilibrium prior to break-up is a crucial concern related to this domain [11]. In this energy domain, the mean field controls the reaction kinetics, and the majority of n-n collisions are Pauli blocked [4,12]. Peripheral collisions result in fragments that resemble projectiles and targets, and fusion-fission events predominate. As the incident energy rises, multifragmentation begins to occur, signaling the end of the fusion processes. A sizable portion of the IMFs in the low energy range (i.e., 40–70 MeV/nucleon) come from the mid-velocity zone [10]. Because of the dynamical fluctuations that rise with incident energy, this kind of pre-equilibrium emission has been hypothesized to be “extended neck” emission. Numerous tests have shown that in these low energy reactions, binary dissipative collisions predominate [5,13].

In this paper, we aim to find the comparison of six different types of secondary fragment formation procedures [14] on the fragment production scenario in low energy i.e. 35MeV/nucleon $^{197}\text{Au}+^{197}\text{Au}$ collisions. The reaction is studied in detail by considering the full colliding geometry. Comparison with experimental data [15] is also done to find the best method. Section 2 describe the model along with various fragment formation techniques. Results and summary are discussed in Sec 3 and 4.

PG Department of Physics, GSSDGS Khalsa
College, Patiala-147001, India
Email: ashuphysics@gmail.com

2. Model

In QMD (n-body) model [4], Hamilton's equations are used by each nucleon to follow classical trajectory. The clusterization algorithms then takes QMD generated phase space as input. The spatial correlation approach, i.e. Minimum Spanning Tree (MST) [4] method identify fragments with nucleons having internucleon distance less than 4 fm. Constraint on relative momenta along with spatial constraint is employed in Minimum Spanning Tree method with Momentum cut (MSTP) [16]. In MSTB(1.1) [17], 4 MeV/nucleon binding energy cut is employed on fragments ($A \geq 3$). But more realistic approach is to apply the energy cut as given in Ref. [18] and is named as MSTB(2.1) [19]. Similarly, the extension of Stimulated Annealing Clusterization Algorithm (SACA(1.1)) [20] is named as SACA(2.1) [21]. We have used all these six approaches to find the fragments and related properties in our present study for of $^{197}\text{Au}+^{197}\text{Au}$ at 35 MeV/nucleon. The brief detail of all the models can be found from the references mentioned with them.

3. Results and Discussion

For the present study we simulated the reactions of $^{197}\text{Au}+^{197}\text{Au}$ at 35 MeV/nucleon over the entire colliding geometry i.e. from $b = 0$ fm to most peripheral geometry i.e. $b = 13$ fm (where $b = b_{\text{max}}$ fm, where $b_{\text{max}} = 1.142(A_p^{1/3} + A_t^{1/3})$; $A_{p/t}$ is the mass of projectile/target). A soft equation of state along with standard energy

dependent n-n cross section is used for the results. The freeze-out time for MST, MSTP, MSTB(1.1) and MSTB(2.1) is taken to be 300 fm/c and it is 60 fm/c for SACA(1.1) and SACA(2.1) as the calculations are performed at a time when heaviest fragment reaches a minima and reabsorption of neighboring smaller fragments occurs afterwards.

Fig. 1 displays the final stage multiplicities of $\langle A^{\text{max}} \rangle$, free nucleons, fragments with mass = 2, light charged particles (LCP's) $2 \leq A \leq 4$, fragments with mass = 4, $5 \leq A \leq 9$, $5 \leq A \leq 20$, $5 \leq A \leq 25$, intermediate mass fragments (IMFs) $5 \leq A \leq 65$, and heavy mass fragments (HMFs) $21 \leq A \leq 65$ as a function of scaled impact parameter. A comparison with different clusterization algorithms (MST, MSTP, MSTB(1.1), MSTB(2.1), SACA(1.1), and SACA(2.1)) is done in this figure. The idea of showing several different mass windows is to identify the different phenomenon that may appear in one mass window but not in other mass ranges. From the figure, we can see that for central and peripheral collisions the final stage multiplicities depend on the clusterization algorithm one is using while its effect nearly vanishes as impact parameter of the reaction rises to maximum. Since at 35 MeV/nucleon energy, the available phase-space is too small to allow the frequent nucleon-nucleon collisions, therefore, no partial fusion is seen for all colliding geometries and $\langle A^{\text{max}} \rangle$ is nearly independent of impact parameter for each clusterization algorithm.

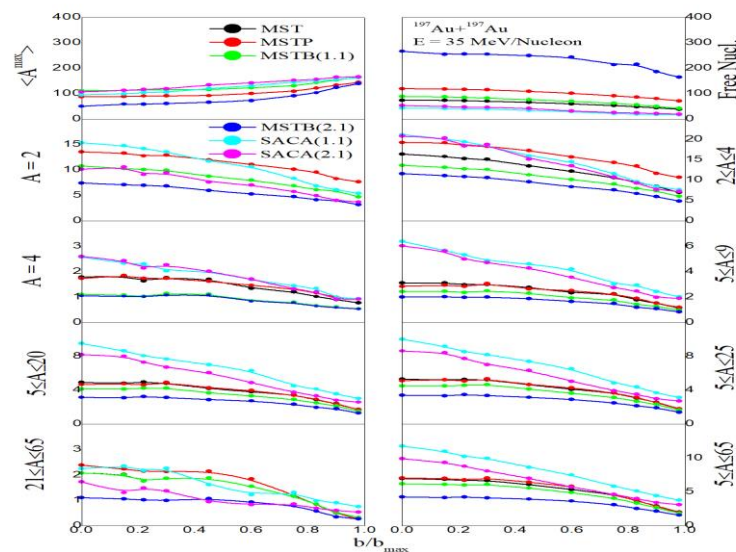


Figure 1. The final stage multiplicities verses reduced impact parameter for different fragment formation techniques. Different colors are used to represent different clusterization methods used for the present study.

Fig. 2 displays the charge distribution sensitivity towards fragment formation techniques at different impact parameters. Solid circles display the experimental data taken from Ref. [15].

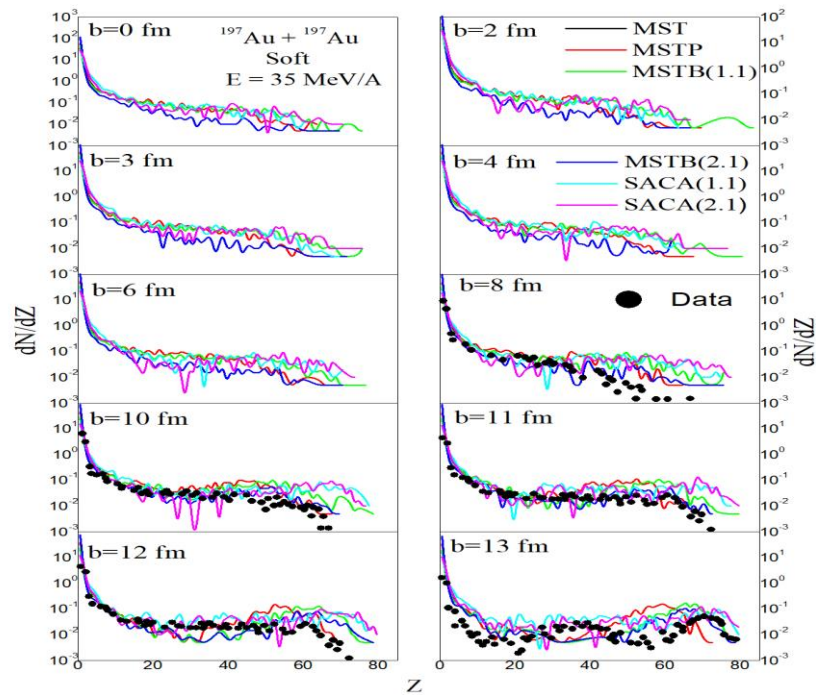
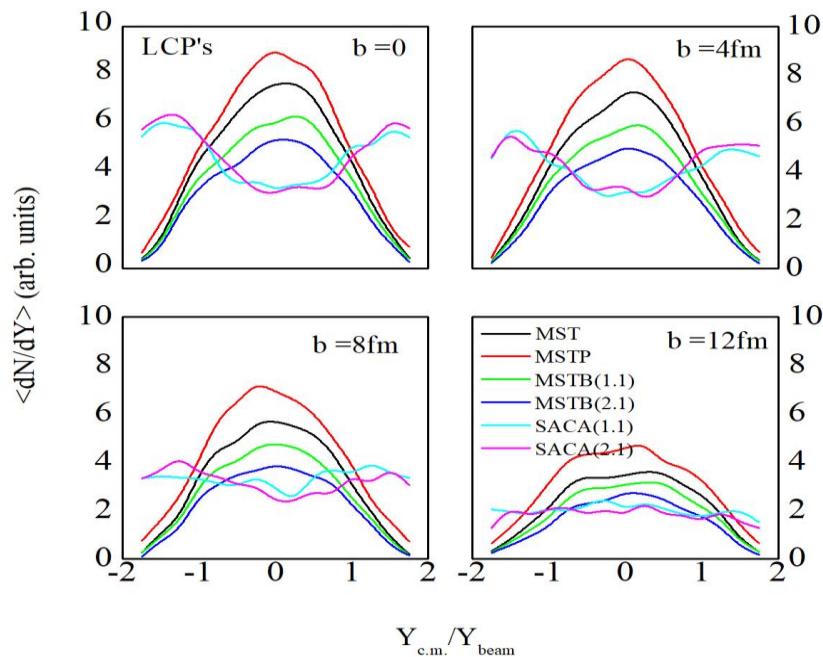


Figure 2. Comparison of the charge distribution for different impact parameters with different fragment formation techniques. Solid black circles represent experimental data [15].

Fig. 3 and 4 displays the information about rapidity distribution of LCPs and IMFs emitted in velocity space. It is clear from the figure that

Interestingly, we see a single continuous curve with negative slope in central collisions whereas it starts following a U-shape with a peak at heavier fusion products for peripheral collisions.

thermalization is better achieved in central collisions rather than peripheral ones.



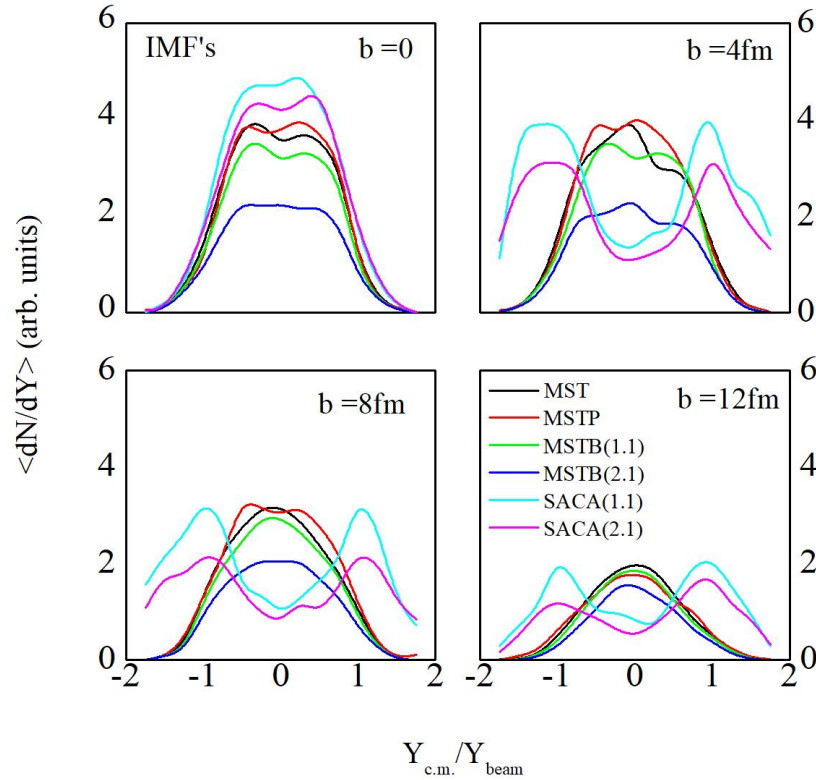


Figure 3 and 4: The rapidity distribution of light charged particles and intermediate mass fragments for $b = 0, 4, 8$ and 12 fm. Comparison is done for different fragment formation techniques.

Moreover, MST, MSTP, MSTB(1.1) and MSTB(2.1) methods predicts the LCP and IMF emission from mid-rapidity area only (as clear from the peak at $Y_{c.m.}/Y_{beam} = 0$) for each impact parameter. On the other hand, SACA(1.1) and SACA(2.1) predicts the contribution from the target and projectile like products apart from the mid-rapidity area. The emission of fragments near target and projectile rapidity reflects that the collisions have binary character [14].

4. Conclusion

Here a comparative study of different fragment formation techniques is done by simulating the reaction of $^{197}\text{Au}+^{197}\text{Au}$ at 35MeV/nucleon over entire colliding geometry. Our results using QMD model coupled with MST, MSTP, MSTB(1.1), MSTB(2.1), SACA(1.1) and SACA(2.1) methods display a clear role of fragment formation techniques on the multiplicity of fragments and rapidity distributions of LCPs and IMFs. The finding highlights the important role of fragment formation criterion in describing the mechanisms of low energy fragmentation process. The SACA versions are clearly better than conventional techniques to recognize the structure of fragments

at low energies.

5. References

- [1] Schütauf A et al 1996 Nucl. Phys. A 607 457
Peaslee G F et al 1994 Phys. Rev. C 49 R2271
Sun R et al 2000 Phys. Rev. C 61 061601 (R)
- [2] Llope W J et al 1995 Phys. Rev. C 51 1325
- [3] Tsang M B et al 1993 Phys. Rev. Lett. 71 1502
- [4] Aichelin J 1991 Phys. Rep. 202 233
Feldmeier H 1990 Nucl. Phys. A 515 147
- [5] Papa M et al 2001 Phys. Rev. C 64 024612
Papa M et al 2005 J. Comput. Phys. 208 403
Bauer W et al 1986 Phys. Rev. C 34 2127
- [6] Bondorf J P et al 1985 Nucl. Phys. A 443 321
Gross D H E 1990 Rep. Prog. Phys. 53 605
- [7] Barz H W et al 1993 Nucl. Phys. A 561 466
Charity R J et al 1988 Nucl. Phys. A 483 371
- [8] Ono A et al 1992 Phys. Rev. Lett. 68 2898
Ono A and Horiuchi H 2004 Prog. Part. Nucl. Phys. 53 501
- [9] Wang L et al 2013 Nucl. Phys. A 920 1
Su J et al 2011 Phys. Rev. C 83 014608

- [10] Zbiri K et al 2007 Phys. Rev. C 75 034612
- [11] Colonna M et al 1995 Nucl. Phys. A 583 525
Garcia-Solis E J and Mignerey A C 1996 Phys. Rev. C 54 276
- [12] Nayak T K et al 1992 Phys. Rev. C 45 132 Sa B H et al 1994 Phys. Rev. C 50 2614
- [13] Molitoris J J et al 1987 Phys. Rev. C 36 220
Berenguer M et al 1992 J. Phys. G: Nucl. Part. Phys. 18 655 Hartnack Ch et al 1998 Eur. Phys. J. A 1 151
- [14] Péter J et al 1995 Nucl. Phys. A 593 95 Toke J et al 1995 Phys. Rev. Lett. 75 2920
- [15] Bougault R et al 1995 Nucl. Phys. A 587 499
Eudes Ph et al 1997 Phys. Rev. C 56 2003
- [16] Vermani Y K and Puri R K 2011 Cent. Eur. J. Phys. 9 621 Kumar R et al 2016 J. Phys. G: Nucl. Part. Phys. 43 025104 Sood S et al 2019 Phys. Rev. C 99 054612
- [17] Milazzo P M et al 1998 Phys. Rev. C 58 953
- [18] Kumar S and Puri R K 1998 Phys. Rev. C 58 320 Singh J et al 2001 Phys. Rev. C 63 054603
- [19] Kumar S and Puri R K 1998 Phys. Rev. C 58 2858 Dhawan J K and Puri R K 2007 Eur. Phys. J. A 33 57 Vermani Y K and Puri R K 2009 J. Phys. G: Nucl. Part. Phys. 36 105103
- [20] Samanta C and Adhikari S 2002 Phys. Rev. C 65 037301
- [21] Samanta C and Adhikari S 2004 Phys. Rev. C 69 049804
- [22] Samanta C and Basu D N 2005 Mod. Phys. Lett. A 20 1605
- [23] Goyal S and Puri R K 2011 Phys. Rev. C 83 047601
- [24] Puri R K et al 1996 Phys. Rev. C 54 R28 Puri R K and Aichelin J 2000 J. Comp. Phys. 162 245
- [25] Vermani Y K et al 2010 J. Phys. G: Nucl. Part. Phys. 37 01510.